Red shift in the photoluminescence of indium gallium arsenide nitride induced by annealing in nitrogen trifluoride

R.L. Woo[a], G. Malouf[b], S.F. Cheng[a], R.N. Woo[a], M. Goorsky[b], R.F. Hicks[a],*

[a]Department of Chemical Engineering, University of California, 5531 Borlter Hall, P.O. Box 951592, Los Angeles, CA 90095, USA
[b]Department of Materials Science and Engineering, University of California, 5531 Borlter Hall, P.O. Box 951592, Los Angeles, CA 90095, USA

Abstract

The effect of annealing a 75nm-thick layer of indium gallium arsenide nitride (InGaAsN) in 1.0×10^{-6} Torr of nitrogen trifluoride (NF_3) has been studied by photoluminescence spectrometry, X-ray diffraction, X-ray photoelectron spectroscopy, and hydrogen adsorption infrared spectroscopy. A red shift of 25 nm in the peak was observed following heating in NF_3 at 530 °C. The compressive strain of the InGaAsN was reduced under annealing in NF_3 ambient, while it increased under annealing in AsH_3 ambient. It is concluded that N atoms diffuse into the alloy during the NF_3 exposure at 530 °C and increase the nitrogen concentration from about 1.2–1.7%.
© 2007 Elsevier B.V. All rights reserved.

1. Introduction

Indium gallium arsenide nitride (InGaAsN) has gained interest in the past decade, because it can be grown lattice matched to GaAs with a band gap in the range of 0.9–1.4 eV [1]. This material has potential applications in multi-junction solar cells, and in long-wavelength solid-state lasers and detectors [2–4]. Nonetheless, its usefulness may be limited by the optical quality of the film. Annealing InGaAsN/GaAs quantum wells (QWs) and superlattices (SLs) in AsH_3 or N_2 has been shown to improve the photoluminescence (PL) by removing non-radiative centers [5,6]. In addition, the heat treatment commonly causes a blue shift in wavelength. This blue shift has been attributed to the interdiffusion of gallium and indium at the InGaAsN/GaAs interface [9–12], to the redistribution of nitrogen on the group V sub-lattice [5,12–14], or to nitrogen out-diffusion [12]. On the other hand, a red shift in the PL emission wavelength after annealing has been observed in only a few cases. Yang et al. [15] and Potter et al. [16] explained the red shift in terms of an increase in the N incorporation in InGaAsN via migration of N from interstitial sites to group V lattice sites. On the other hand, Balkan et al. [17] explained it in terms of hydrogen-induced chemical effects.

The aim of this work is to investigate the influence of nitrogen trifluoride (NF_3) annealing directly on the properties of InGaAsN layer, not InGaAsN/GaAs QWs and SLs. In our research, NF_3 is the nitrogen source for growing InGaAsN by metalorganic chemical vapor deposition [19]. After annealing in NF_3, we have recorded a red shift of 5–25 nm in the PL spectrum. Characterization of the material by high-resolution X-ray diffraction (XRD), X-ray photoelectron spectroscopy (XPS), and hydrogen adsorption infrared spectroscopy (IR) suggests that the red shift results from nitrogen diffusion into the bulk film.

2. Experimental methods

InGaAsN films of 75 nm thickness were grown on GaAs (0 0 1) substrates in a Veeco D125 metalorganic chemical

---

*Corresponding author. Tel.: +1 310 206 6865; fax: +1 310 206 4107.
E-mail address: rhicks@ucla.edu (R.F. Hicks).

vapor deposition reactor. The following conditions were used during growth: 550 °C, 60 Torr hydrogen, 0.2 mTorr trimethylindium (TMIn), 6.1 mTorr of trimethylgallium (TMGa), 21.6 mTorr of tertiarybutylarsine (TBAs), 12.0 mTorr NF_3 (V/III ratio of 5.3), and a total flow rate of 37 L/min of hydrogen (at 25 °C and 760 Torr). Once growth was completed, the TBAs and the hydrogen flows were maintained until the sample was cooled down to 300 and 24 °C, respectively. Then, the sample was transferred to an ultrahigh vacuum chamber without air exposure. In vacuum, the samples were annealed in 1.0×10^{-6} Torr of NF_3 between 250 and 530 °C for 1 hr. The equivalent of 3600 Langmuir (L) ($1 L = 1 \times 10^{-6}$ Torr s) of NF_3 was exposed to the alloy surface during each exposure.

The surface composition of the film was identified by XPS before and after anneal without air exposure. Core level photoemission spectra of the In 3d, Ga 2p, As 3d, and N 1s lines were collected with a PHI 3057 spectrometer using magnesium Kα X-rays ($hv = 1286.6$ eV). All XPS spectra were taken in small area mode with a 7° acceptance angle and 23.5 eV pass energy. The detection angle with respect to the surface normal was 25°. The surface composition was determined from the integrated intensity of the In 3d, Ga 2p, As 3d, and N 1s photoemission peaks, dividing by their sensitivity factors, 4.36, 3.72, 0.68 and 0.48, respectively. Infrared spectra of adsorbed hydrogen were recorded on a Bio-Rad FTS-40A instrument, using an internal reflection technique that has been described elsewhere [18]. The XRD measurements were acquired on a Bede D^3 high-resolution diffractometer using Cu Kα X-rays. PL measurements were performed on a Phillips PLM 100 spectrometer using the 488 nm line of an argon laser.

3. Results

Annealing in NF_3 significantly changes the PL response. Shown in Fig. 1 are low-temperature (77 K) PL spectra of the InGaAsN after treatment at different temperatures. Temperatures greater than 530 °C were not investigated due to equipment limitations. The peak at 822 nm is due to
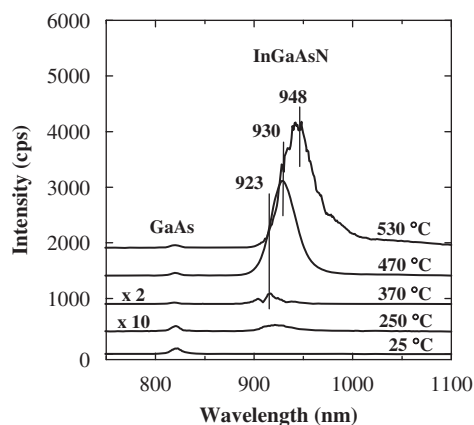
the GaAs substrate. The longer-wavelength peaks (923–948 nm, depending on annealing temperature) are due to InGaAsN. The annealing affects the PL in two ways. One is a strong enhancement of the radiative efficiency, which is commonly observed in annealing studies [5–16]. The other is a red shift of the InGaAsN peak position from 923 nm at 370 °C to 948 nm at 530 °C.

Shown in Fig. 2 are X-ray $\omega - 2\theta$ measurements around the (0 0 4) GaAs peak of the annealed samples. The sharp peak at 0 arcsec is due to the GaAs substrate and the broad shoulder on the left and the related fringes are due to the thin 75 nm InGaAsN epilayer. A gradual change of this peak position is seen from about -200 arcsec for annealing at 250 °C to -110 arcsec for annealing at 530 °C.

Presented in Table 1 is the surface composition of the InGaAsN epilayer at different treatment temperatures. Since the number of photoelectrons detected by XPS decreases exponentially with depth, a surface rich in one element (i.e., arsenic) would tend to over-emphasize the abundance of this species relative to the other elements in the film. Note that there is very little change in the distribution of surface species during heating from 25 to 370 °C. At 470–530 °C, the surface nitrogen concentration jumps from 11.5 to $19.5 \pm 1.4\%$, while the arsenic concentration decreases from 60.0 to $49.0 \pm 2.1\%$. Overall, the group V surface concentration remains constant at 70.0%, and no significant change occurs in the gallium and indium concentrations during annealing. These results indicate that arsenic desorbs from the semiconductor surface and is replaced by nitrogen upon heating the material in NF_3 above 400 °C [20].

For comparison, we have performed the annealing experiment in 1×10^{-6} Torr AsH_3. Shown in Fig. 3 are X-ray $\omega - 2\theta$ measurements of an as-grown sample, a sample that has been heated in NF_3 to 530 °C and a sample that has been heated in AsH_3 at 530 °C. Note that the samples used in this set contain a 225-nm-thick InGaAsN layer, which is $3\times$ the thickness of the InGaAsN films examined in Fig. 2. The (0 0 4) InGaAsN peak on the left of
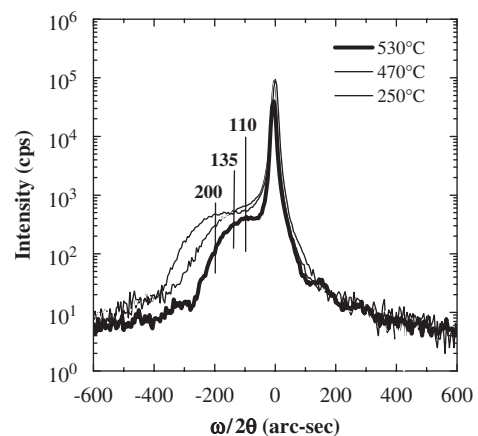

Fig. 1. Photoluminescence spectra of InGaAsN before and after a 1 hr anneal at different temperatures in 1.0×10^{-6} Torr NF_3.

Fig. 2. The (0 0 4) X-ray rocking curve spectra for InGaAsN before and after a 1 hr anneal at different temperatures in 1.0×10^{-6} Torr NF_3.

Table 1
The amount of In, Ga, As, and N atoms observed by XPS on InGaAsN surface after 3600 L (1×10^{-6} Torr.s) of NF$_3$ exposure at different temperatures

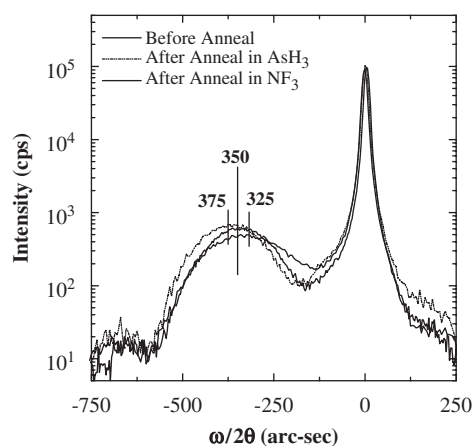| Temperature (°C)	In (%)	Ga (%)	As (%)	N (%)	N/V
24	1.9±0.5	26.0±1.6	63.1±2.1	9.0±1.4	0.12±0.03
250	1.8±0.5	24.8±1.6	61.7±2.1	11.7±1.4	0.16±0.03
370	2.1±0.5	26.2±1.6	60.3±2.1	11.5±1.4	0.16±0.03
470	3.1±0.5	27.7±1.6	50.2±2.1	19.0±1.4	0.27±0.03
530	2.4±0.5	29.3±1.6	48.0±2.1	20.3±1.4	0.30±0.03

Fig. 3. The (0 0 4) X-ray rocking curve spectra for InGaAsN before and after a 1 hr anneal at 530 °C in 1.0×10^{-6} Torr NF$_3$ and AsH$_3$.

the (0 0 4) GaAs substrate peak looks better resolved compared to the InGaAsN peak in Fig. 2, due to (i) thickness and (ii) difference in initial composition. In addition, the thickness fringes can be observed in Fig. 3. The peak position at −350 arcsec as opposed to −200 arc-sec may be due to the composition changes within the sample. These samples were grown at the same time and X-ray $\omega-2\theta$ measurements were taken to confirm that they had similar starting parameters (same peak position and intensity) before heat treatment. Heat treatment was carried out for 1 hr at 530 °C. It is seen that the peak for the InGaAsN film shifts −25 arcsec after heating in AsH$_3$, while it shifts +25 arcsec after heating in NF$_3$. These data clearly show that the gas ambient during annealing causes reproducible changes in the bulk composition of the InGaAsN film.

The composition of the InGaAsN film was calculated using the Vegard's law, Moon's method, the XRD peak position from Fig. 2, and the PL data from Fig. 1. The band gap of GaAs, GaN, InAs, and InN used in this calculation are 1.424, 3.2, 0.354, and 1.97 eV, respectively [22,23]. The bowing parameters of InGaN, InGaAs, GaAsN, and InAsN used in this calculation are 1.621, 0.672, 7.494, and 5.433, respectively [24]. From the critical thickness calculation, we found the critical thickness to be around 80 nm. Assuming the film was strained, we

calculated that after the NF$_3$ anneal at 250 and 530 °C, the composition of the 75-nm-thick film changed from In$_{0.045}$Ga$_{0.955}$As$_{0.988}$N$_{0.012}$ to In$_{0.05}$Ga$_{0.95}$As$_{0.983}$N$_{0.017}$, i.e., an increase in nitrogen content from 1.2% to 1.7%. Note that the samples from Fig. 3 are well beyond the critical thickness and we continue to see similar peak shifts.

Presented in Fig. 4 are infrared spectra of adsorbed hydrogen on the InGaAsN (0 0 1) surface before and after annealing in NF$_3$ at 530 °C. Bands in the frequency ranges associated with the As–H and N–H stretching vibrations are shown in (a) and (b), respectively. Only As–H absorption peaks at 2135, 2100, 2090, 2050, 2020 cm^{-1} are observed after growth. These same bands have been observed for As-rich GaAs (0 0 1), where the surface is completely terminated with arsenic dimers [20]. After heating in NF$_3$, the peak area under the As–H absorption bands was reduced by 24.3%, while at the same time, one or two N–H stretching modes appeared between 3300 and 3000 cm^{-1}. The stretching modes in this frequency range correspond to the symmetric and asymmetric stretching modes of NH$_2$ and/or NH. Note that a broad Ga–H absorption band was observed on the annealed sample, but it is not presented in the figure. The changes in surface composition recorded by infrared spectroscopy are in agreement with the photoemission data reported in Table 1. After exposure to NF$_3$ at 530 °C, a 23.8% reduction in As concentration is obtained by XPS compared to a 24.3% reduction recorded in the area of the As–H infrared bands.

4. Discussion

In previous studies, the PL efficiency of InGaAsN/GaAs QW and SL has been greatly increased by rapid thermal annealing (less than a few minutes), slow thermal annealing (greater than 5 min), and laser spot heating in either N$_2$ or AsH$_3$. In few cases where heating was carried out above 650 °C, the PL efficiency was reduced due to surface degradation. The improvement in PL efficiency after heat treatments is attributed to a reduction of non-radiative centers associated with the nitrogen incorporation [5,6]. Aside from improving PL efficiency, the heat treatments usually shift the emission to lower wavelengths. Yang et al. [15] and Potter et al. [16] did observe a red shift in the emission. The difference between their approaches and the other studies was the noticeably lower growth and heat treatment temperatures 460–500 and 200–550 °C, respectively [16].

In our work, a large increase in the PL intensity from InGaAsN layer is observed after NF$_3$ annealing. In addition, a shift to longer wavelengths is observed as shown in Fig. 1. The shift is 7 nm after heating to 470 °C and 25 nm after heating to 530 °C. Note that a 25 nm is equivalent to a 35.6 meV change in band gap. The shift in PL emission to longer wavelengths may be due to an increase in the bulk nitrogen concentration [15,16,22], a decrease in the bulk gallium concentration (fluorine etching of group III elements), or both. Another possibility might
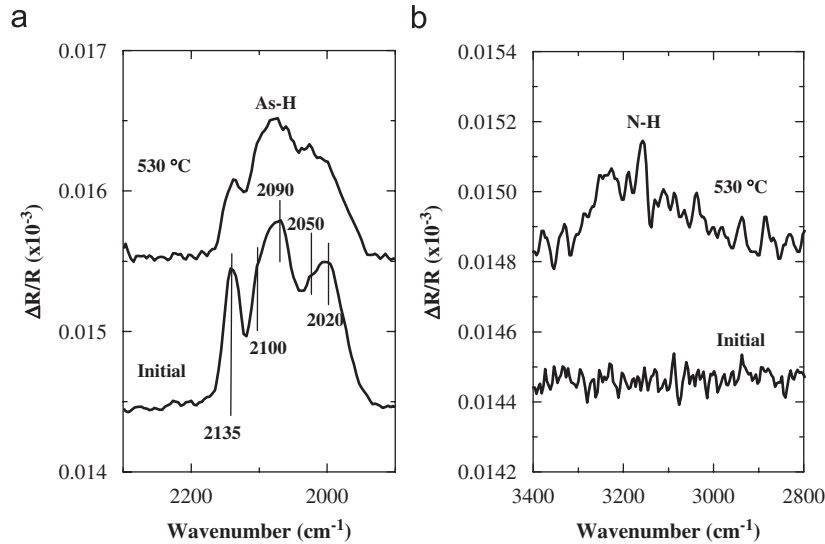
Fig. 4. Infrared reflectance spectra of adsorbed hydrogen on InGaAsN before and after a 1 h anneal at 530 °C in 1.0×10^{-6} Torr NF_3: (a) As–H stretching modes and (b) N–H stretching modes.

be that the N atom migrates from interstitial sites to As sites [14–16].

In the X-ray diffraction spectrum (Fig. 2), we see a positive peak shift with increasing annealing temperature, meaning that the InGaAsN epilayer becomes more closely lattice matched to the GaAs substrate. There are two possible mechanisms for reducing the compressive strain: substitution of nitrogen for arsenic in the bulk film, or substitution of gallium for indium in the bulk film by solid-state diffusion. Mechanism 2 contradicts the PL results, so this leaves mechanism 1 as the only likely explanation.

The XPS and infrared data (Table 1 and Fig. 4) support the conclusion that nitrogen is diffusing into the InGaAsN film. These results show that after annealing in NF_3, the coverage of N atoms on the surface has increased from 9% to 20% of the group V sites. Above 400 °C, arsenic desorbs from the surface and the amount of desorption increases with temperature [20]. This allows NF_3 to adsorb onto the unoccupied group V sites. During the course of annealing, arsenic continues to desorb, providing a pathway for arsenic to diffuse out of the bulk film, following a vacancy diffusion mechanism [21]. Nitrogen atoms at the surface can then diffuse into the bulk, making use of bulk group V vacancies. Alternatively, when arsenic is supplied to the surface during annealing in AsH_3, the arsenic coverage increases, while the nitrogen atom coverage decreases. This reverses the solid-state diffusion process, with N atoms moving out of the bulk and As atoms moving in.

In order to gain some insight on the depth uniformity of N concentration, we used the Bede RADS Mercury to simulate the experimental XRD data. Shown in Fig. 5 are X-ray data of annealed sample at 250 °C and simulations predicted by RADS using single layer and four layers, where the overall thickness was kept around 75 nm. Strong
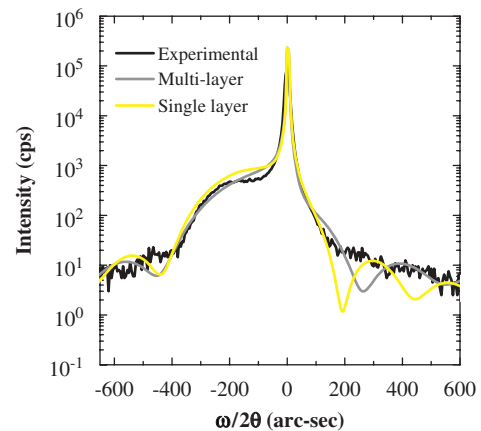

Fig. 5. Experimental X-ray diffraction data for InGaAsN annealed at 250 °C compared with simulations assuming single uniform layer and four multi-layers.

fringes are present in the simulation for a single uniform layer and do not change much when a thin layer of N-rich InGaAsN is added. On the other hand, they tend to smooth out as more layers are added in the simulation. Based on these preliminary fittings, the N introduced through annealing is not uniformly distributed in the layer or being concentrated in the first few monolayers. We believe that the annealed film is graded, where the N concentration at the surface is the highest.

In summary, our results show that annealing InGaAsN in NF_3 at temperatures above 450 °C drives nitrogen into the bulk, causing the alloy to be more closely lattice matched to GaAs. At the same time, the annealing improves the optical emission properties of the film. The results presented here suggest that by using a mixture of AsH_3 and NF_3, one can precisely control the change in lattice constant of the InGaAsN during annealing.

Acknowledgments

References

[1] M. Kondow, K. Uomi, A. Niwa, T. Kitatani, S. Watahiki, Y. Yazawa, Jpn. J. Appl. Phys. 35 (Part 1) (1996) 1273.

[2] J.S. Harris Jr., Semicond. Sci. Technol. 17 (2002) 880.

[3] J.F. Geisz, D.J. Friedman, Semicond. Sci. Technol. 17 (2002) 769.

[4] M. Pessa, C.S. Peng, T. Jouhti, E.M. Pavelescu, W. Li, S. Karirinne, H. Liu, O. Okhotnikov, IEEE Proc. Optoelectron. 150 (2003) 12.

[5] M. Kondow, T. Kitatani, S. Shirakata, J. Phys.: Condens. Matter 16 (2004) S3229.

[6] L. Largeau, C. Bondoux, G. Patriarche, Appl. Phys. Lett. 79 (2001) 1795.

[7] E.V. Rao, A. Ougazzaden, Y. Le Bellego, M. Juhel, Appl. Phys. Lett. 72 (1998) 1409.

[8] R. Bhat, C. Caneau, L. Salamanca-Riba, W. Bi, C. Tu, J. Crystal Growth 195 (1998) 427.

[9] H.P. Xin, C.W. Tu, M. Geva, Appl. Phys. Lett. 75 (1999) 1416.

[10] W. Lei, J. Turpeinen, P. Melanen, P. Savolainen, P. Ususimaa, M. Pessa, Appl. Phys. Lett. 78 (2001) 91.

[11] C.S. Peng, E.M. Pavelescu, T. Jouhti, J. Konttinen, I.M. Fodchuk, Y. Kyslovsky, M. Pessa, Appl. Phys. Lett. 80 (2002) 4720.

[12] M. Albrecht, V. Grillo, T. Remmete, H.P. Strunk, Appl. Phys. Lett. 81 (2002) 2719.

[13] J.M. Chauveau, A. Trampert, K.H. Ploog, Appl. Phys. Lett. 84 (2004) 2503.

[14] A. Jenichen, C. Engler, G. Leibiger, V. Gottschalch, Surf. Sci. 574 (2005) 144.

[15] X. Yang, J.B. Heroux, M.J. Jurkovic, W.I. Wang, J. Vac. Sci. Technol. B 17 (1999) 1144.

[16] R. Potter, S. Mazzucato, N. Balkan, M.J. Adams, Superlattices Microstruct. 29 (2001) 169.

[17] N. Balkan, S. Mazzucato, A. Erol, C.J. Hepburn, R.J. Potter, A. Boland-Thoms, A.J. Vickers, P.R. Chalker, T.B. Joyce, T.J. Bullough, IEE Proc.—Optoelectron. 151 (2004) 284.

[18] G. Chen, S.F. Cheng, D.J. Tobin, L. Li, K. Raghavachari, R.F. Hicks, Phys. Rev. B 68 (2003) 121303.

[19] S.F. Cheng, R.L. Woo, A.M. Noori, G. Malouf, M.S. Goorsky, R.F. Hicks, J. Crystal Growth 299 (2) (2007) 277.

[20] Q. Fu, L. Li, C.H. Li, M.J. Begarney, D.C. Law, R.F. Hicks, J. Phys. Chem. B 104 (2000) 5595.

[21] Q. Fu, L. Li, R.F. Hicks, Phys. Rev. B 61 (2000) 11034.

[22] K. Kassali, N. Bouarissa, Solid State Electron. 44 (2000) 501.

[23] ⟨http://www.ioffe.rssi.ru/SVA/NSM/Semicond/index.html⟩.

[24] M. Ferhat, Phys. Stat. Sol. B 241 (10) (2004) R38.